ORIGINAL ARTICLE

Cancer Science WILEY

M2-like tumor-associated macrophages promote epithelial–mesenchymal transition through the transforming growth factor β/Smad/zinc finger e-box binding homeobox pathway with increased metastatic potential and tumor cell proliferation in lung squamous cell carcinoma

Ryota Sumitomo[1,2] 🔘 | Toshi Menju[1] | Yumeta Shimazu[1] | Toshiya Toyazaki[1] | Naohisa Chiba[1] | Hideaki Miyamoto[1] | Yutaka Hirayama[3] | Shigeto Nishikawa[1] | Satona Tanaka[1] | Yojiro Yutaka[1] | Yoshito Yamada[1] | Daisuke Nakajima[1] | Akihiro Ohsumi[1] | Masatsugu Hamaji[1] | Atsuyasu Sato[3] | Akihiko Yoshizawa[4] | Cheng-Long Huang[2] | Hironori Haga[4] | Hiroshi Date[1]

[1]Department of Thoracic Surgery, Graduate School of Medicine, Kyoto University, Kyoto, Japan

[2]Department of Thoracic Surgery, Tazuke Kofukai Medical Research Institute, Kitano Hospital, Osaka, Japan

[3]Department of Respiratory Medicine, Graduate School of Medicine, Kyoto University, Kyoto, Japan

[4]Department of Diagnostic Pathology, Kyoto University Hospital, Kyoto, Japan

Correspondence
Toshi Menju, Department of Thoracic Surgery, Graduate School of Medicine, Kyoto University, Kyoto, 606-8507, Japan.
Email: toshimnj@kuhp.kyoto-u.ac.jp

Funding information
Japan Society for the Promotion of Science, Grant/Award Number: 20H03770

Abstract

Epithelial-mesenchymal transition (EMT) promotes primary tumor progression toward a metastatic state. The role of tumor-associated macrophages (TAMs) in inducing EMT in lung squamous cell carcinoma (LUSC) remains unclear. We aimed to clarify the significance of TAMs in relation to EMT in LUSC. We collected 221 LUSC specimens from patients who had undergone surgery. Immunohistochemistry was performed to evaluate M1-like and M2-like TAM distribution and EMT by E-cadherin and vimentin staining. Human LUSC cell lines (H226 and EBC-1) and a human monocyte cell line (THP-1) were used for in vitro experiments. M2-like polarization of TAMs and EMT marker expression in LUSC cells were evaluated by western blotting. The biological behavior of LUSC cells was evaluated by migration, invasion, and cell proliferation assays. Immunohistochemical analysis showed that 166 (75.1%) tumors were E-cadherin-positive and 44 (19.9%) were vimentin-positive. M2-like TAM density in the tumor stroma was significantly associated with vimentin positivity and worse overall survival. Western blotting demonstrated higher levels of CD163, CD206, vascular endothelial growth factor, and transforming growth factor beta 1 (TGF-β1) in TAMs versus unstimulated macrophages. Furthermore, increased TGF-β1 secretion from TAMs was confirmed by ELISA. TAM-co-cultured H226 and EBC-1 cells exhibited EMT (decreased E-cadherin, increased vimentin). Regarding EMT-activating

---

------

transcriptional factors, phosphorylated Smad3 and ZEB-family proteins were higher in TAM-co-cultured LUSC cells than in parental cells. TAM-co-cultured H226 and EBC-1 cells demonstrated enhanced migration and invasion capabilities and improved proliferation. Overall, the present study suggests that TAMs can induce EMT with increased metastatic potential and tumor cell proliferation in LUSC.

KEYWORDS
E-cadherin, epithelial–mesenchymal transition, lung squamous cell carcinoma, tumor-associated macrophage, vimentin

1 | INTRODUCTION

Lung squamous cell carcinoma (LUSC), an important subtype of non-small cell lung cancer, accounts for approximately 30% of patients with non-small cell lung cancer.[1] Despite the development of novel therapies for lung cancer, such as molecular-targeted therapies and immune checkpoint inhibitors,[2] treating LUSC remains a challenge. Molecular-targeted therapies, including epidermal growth factor receptor tyrosine kinase inhibitors and anaplastic lymphoma kinase inhibitors, are not applied for LUSC because most patients with advanced LUSC do not carry mutations in driver genes. Furthermore, immune checkpoint inhibitors, such as programmed death-ligand 1 inhibitors, exhibit less efficacy in patients with programmed death-ligand 1-negative tumors.[3] Chemotherapy remains the mainstay of treatment for advanced LUSC patients.[4] Therefore, further clarifying the tumor biology of LUSC to identify new therapeutic targets is necessary.

Tumor-associated macrophages (TAMs) are key tumor microenvironment components that influence tumor progression.[5–7] Generally, macrophages are polarized into separate phenotypes, such as the tumor-suppressing M1 and tumor-promoting M2 phenotypes, depending on the physiological or pathological condition.[8–10] Several experimental studies have demonstrated that TAMs can promote epithelial-mesenchymal transition (EMT),[11] by which tumor cells disseminate from the primary lesion toward a metastatic site, leading to a poor prognosis.[12] During EMT, a decrease in the expression of epithelial markers, such as E-cadherin, and an increase in the expression of mesenchymal markers, such as vimentin, occur through the upregulation of EMT-transcription factors, including zinc finger e-box binding homeobox (ZEB) 1, ZEB2, Snail, Slug, and twist family basic helix–loop–helix transcription factor (TWIST).[13] Furthermore, epigenetic, transcriptional, and microRNA regulators that directly or indirectly regulate EMT have been identified.[14] EMT in tumor cells can be induced by various cytokines, such as transforming growth factor beta (TGF-β) via the TGF-β/Smad pathway and Wnt ligands via the canonical and non-canonical Wnt signaling pathways.[15,16] Indeed, Alonso-Nocelo et al. reported that EMT can be induced by co-culturing A549 human lung adenocarcinoma cells with THP-1 human monocytes, although the underlying mechanism was not investigated.[17]

In the context of squamous cell carcinoma, the influence of TAMs on EMT appears to be more complex. While some experimental studies have revealed that M2-like TAMs can promote EMT in certain types of squamous cell carcinoma, such as laryngeal squamous cell carcinoma, head and neck squamous cell carcinoma, and esophageal squamous cell carcinoma,[18–21] other studies have suggested that M1-like TAMs can promote EMT in oral squamous cell carcinoma via the IL6/Stat3/THBS1 feedback loop.[22] Overall, there is a lack of consensus regarding the exact impact of TAMs on EMT in different types of squamous cell carcinoma. Furthermore, the impact of TAMs on EMT in LUSC remains unclear.

The present clinical and experimental study using an in vitro model with THP-1 cells was performed to elucidate the biological significance of TAMs in relation to EMT in LUSC in consideration of the abovementioned findings.

2 | MATERIALS AND METHODS

2.1 | Patients

A total of 221 LUSC specimens were collected from patients who had undergone surgery at the Kyoto University Hospital from June 2003 to March 2015. The study was approved by the ethics committee of the hospital (approval no. R1706), and written informed consent was provided by each patient. Patients who had received neoadjuvant therapy, had undergone noncurative surgery, or had multiple cancers were excluded. All specimens were subjected to tissue microarray (TMA) analysis, as described below. The tumors were staged using the eighth tumor node metastasis classification system.[23] The histological type and the differentiation grade of the tumors were determined according to the classification system developed by the World Health Organization.[24] The patients' medical records and histopathological diagnoses were thoroughly documented. The patient records contained follow-up data until November 2022. The overall median follow-up interval was 59.6 months.

2.2 | Tissue microarray

Tissue microarrays were made by the pathologists in the Department of Diagnostic Pathology at Kyoto University Hospital using a similar approach to that previously reported by Kononen et al.[25] Tissues were fixed in 10% neutral-buffered formalin for 24 h before

being embedded in paraffin. Briefly, after the case selection described above, paraffin-embedded tumor blocks with sufficient tissue were selected for TMA. The most representative regions of the tumors were selected based on the morphology of the H&E-stained slide. Tissue cores measuring 2 mm in diameter were punched out from each donor tumor block, using thin-walled stainless steel needles (Azumaya Medical Instruments), and were arrayed in a recipient paraffin block. Non-neoplastic lung tissue cores from selected patients were arrayed in the same block as negative controls.

2.3 | Immunohistochemistry

Immunohistochemical studies were performed to examine M1-like TAM distribution by inducible nitric oxide synthase (iNOS) staining, M2-like TAM distribution by CD163 staining, and EMT by E-cadherin and vimentin staining following the recommended protocol, using the Ventana BenchMark GX system (Ventana Medical Systems) or manually. The following antibodies were prepared: rabbit polyclonal anti-human iNOS (#ab3523; 1:50; Abcam), mouse monoclonal anti-human CD163 (#760–4437; prediluted; Ventana Medical Systems), mouse monoclonal anti-human E-cadherin (#PA0387; 1:300; Leica Biosystems), mouse monoclonal anti-human vimentin (#NCL-L-VIM-572; 1:300; Leica Biosystems), rabbit monoclonal anti-human phosphorylated Smad3 (pSmad3; #9520; 1:100; Cell Signaling Technology), rabbit monoclonal anti-human ZEB1 (#ab203829; 1:50; Abcam), and rabbit monoclonal anti-human ZEB2 (#ab230561; 1:500; Abcam).

Formalin-fixed paraffin-embedded tissues were cut into 4-μm sections and mounted onto poly-L-lysine-coated slides. After deparaffinization and rehydration, antigen retrieval was conducted with Cell Conditioner 1 (Ventana Medical Systems) for 32 min at 100°C against iNOS and CD163 and for 60 min at 100°C against ZEB1 and ZEB2, or with a microwave for 20 min in 10 μmol/L citrate buffer solution at pH 6.0 against E-cadherin, vimentin, and pSmad3. Subsequently, the sections were incubated with specific primary antibodies: iNOS (32 min at 37°C), CD163 (16 min at 37°C), E-cadherin (overnight at room temperature), vimentin (overnight at room temperature), ZEB1 (60 min at 37°C), ZEB2 (60 min at 37°C), and pSmad3 (overnight at room temperature). The sections were then incubated with OptiView HQ Linker (Ventana Medical Systems) for 8 min at 37°C and OptiView HRP Multimer (Ventana Medical Systems) for 8 min at 37°C against iNOS, CD163, ZEB1, and ZEB2, or incubated with biotinylated secondary antibody for 1 h, followed by incubation with the avidin–peroxidase complex for 1 h, against E-cadherin, vimentin, and pSmad3 and then visualized with 3,3′-diaminobenzidine tetrahydrochloride (Dojindo Laboratories). Lastly, counterstaining was performed with Mayer's hematoxylin.

The TMA slides were scanned to obtain the whole slide images. The iNOS-positive and CD163-positive cells were counted using QuPath version 0.4.0 (open-source bioimage analysis software), and the density of iNOS-positive or CD163-positive macrophages in the tumor stroma or islets was respectively determined as the number of cells per mm^2 (Figure S1). Receiver operating characteristic curve

analysis was performed, and survival was predicted by comparing the area under the curve to determine the optimal cut-off value with maximal sensitivity and specificity for respective TAM density. If there was no association with survival, the cut-off value was set at the median.

Immunohistochemical expression of E-cadherin, vimentin, pSmad3, ZEB1, and ZEB2 was evaluated in four distinct fields with a minimum of 500 cells by two investigators (RS and TM) without knowledge of the patients' clinical information. Discordant cases were jointly reviewed until a consensus was reached. The proportion of positive cells was measured and classified as 0 (no staining), +1 (weak), +2 (moderate), and +3 (strong), and each specimen was categorized as negative (0, +1) or positive (+2, +3), as previously reported.[26]

2.4 | Cell culture and reagents

Cell lines of human LUSC, H226 (ATCC) and EBC-1 (Riken BioResource Center), and human monocyte, THP-1 (Japanese Collection of Research Bioresources Cell Bank), were obtained and cultured in RPMI 1640 medium (Sigma-Aldrich) supplemented with 10% heat-inactivated FBS (HyClone, Thermo Fisher Scientific K.K.) and penicillin/streptomycin in a humidified atmosphere with 5% CO_2 at a constant temperature of 37°C. All cell lines were tested for mycoplasma with the MycoAlert Mycoplasma Detection Kit (Lonza), and mycoplasma negativity was confirmed before use.

2.5 | Macrophage generation and differentiation

THP-1 cells were first treated with 100 ng/mL phorbol 12-myristate 13-acetate (Abcam) for 24 h to generate unstimulated macrophages, followed by incubation with IL-4 (50 ng/mL, PeproTech) and IL-13 (20 ng/mL, PeproTech) for 48 h for differentiation into M2-like macrophages.

2.6 | Generation of tumor-associated macrophages

Co-culture was performed in a six-well Transwell system (0.4 μm pore size, Corning). Briefly, 2.0×10^6 unstimulated macrophages were suspended in 2.5 mL and seeded into the lower well, while 1.5×10^5 LUSC cells (H226 or EBC-1) were suspended in 1.5 mL and plated in the upper chamber. After 48 h of co-culture, the macrophages in the lower well were harvested as TAMs.

2.7 | Generation of lung squamous cell carcinoma cells co-cultured with tumor-associated macrophages

Co-culture was performed in a six-well Transwell system (0.4 μm pore size, Corning). Briefly, 2.5×10^5 LUSC cells (H226 or EBC-1) were suspended in 2.5 mL and seeded into the lower well, while 1.2×10^6 cells of respective TAMs were suspended in 1.5 mL and

plated in the upper chamber. After 48h of co-culture, the LUSC cells in the lower well were harvested.

2.8 | Tumor-associated macrophage-conditioned medium

In brief, 8.0×10^5 TAMs per 1 mL were cultured in RPMI 1640 containing 10% FBS for 48h to obtain the conditioned medium, which was centrifuged at 2000g for 10min to remove suspended cells. The supernatant was collected, and the same volume of RPMI 1640 containing 10% FBS was added to reconstitute the TAM-conditioned medium.

2.9 | Cell proliferation assay

The experiments were performed using a 24-well Transwell system (0.4μm pore size, Corning). Briefly, 3.5×10^4 LUSC cells (H226 or EBC-1) were suspended in 700μL and plated in the lower well, while 8.0×10^4 TAMs were suspended in 100μL and seeded into the upper chamber. As a control, 3.5×10^4 LUSC cells were suspended in 700μL and plated in wells without the upper chamber. After 24, 48, 72, or 96h of co-culture, the upper chamber was removed, and 70μL Cell Counting Kit-8 reagent (Dojindo Laboratories) was added into the well. After 1h at 37°C, the absorbance at a wavelength of 450nm was measured using Microplate Manager 6 (Bio-Rad Laboratories). All experiments were performed in triplicate.

2.10 | Migration and invasion assay

The migration and invasion assay was performed using a 24-well Transwell system (8.0μm pore size, Corning). For the migration assay, 2.5×10^4 LUSC cells (H226 or EBC-1) co-cultured with TAMs were suspended in 500μL RPMI 1640 containing 1% FBS and seeded into the upper chamber, with the lower well filled with 750μL of the abovementioned TAM-conditioned medium. As a control, 2.5×10^4 parental LUSC cells were suspended in 500μL RPMI 1640 containing 1% FBS and seeded into the upper chamber, with the lower well filled with 750μL RPMI 1640 containing 10% FBS. After incubation for 20h, cells were fixed in methanol, and the number of cells that transmigrated through the chamber filter to the lower surface of the filters was counted manually by staining with Diff-Quick (Sysmex). For the invasion assay, the upper chamber was coated with Matrigel (Biocoat, Corning). The remaining steps were conducted as described for the migration assay. Each experiment was performed in triplicate.

2.11 | Western blotting

Protein was lysed in radioimmunoprecipitation buffer containing protease inhibitors at 4°C for 30min to obtain whole cell lysates.

Lysates were resolved by 10–15% SDS-PAGE and transferred onto Immobilon-P PVDF membranes (Millipore). Blots were incubated overnight at 4°C with primary antibodies: anti-CD163 (#ab19518; Abcam), anti-CD206 (#91992; Cell Signaling Technology), anti-E-cadherin (#3195; Cell Signaling Technology), anti-vimentin (#5741; Cell Signaling Technology), anti-pSmad3 (#9520; Cell Signaling Technology), anti-TGF-β1 (#ab92486; Abcam), anti-vascular endothelial growth factor (VEGF)-A (#sc-152; Santa Cruz Biotechnology), anti-Wnt1 (#sc-5630; Santa Cruz Biotechnology), anti-Wnt2b (#sc-7382; Santa Cruz Biotechnology), anti-Wnt3 (#sc-74,537; Santa Cruz Biotechnology), anti-Wnt5a (#sc-23,698; Santa Cruz Biotechnology), anti-CaMKII (#4436; Cell Signaling Technology), anti-phospho-CaMKII (#12716; Cell Signaling Technology), anti-Snail (#3879; Cell Signaling Technology), anti-Slug (#9585; Cell Signaling Technology), anti-TWIST (#46702; Cell Signaling Technology), anti-ZEB1 (#ab203829; Abcam), anti-ZEB2 (#97885; Cell Signaling Technology), and anti-β-actin (#A5441; Sigma-Aldrich). Membranes were incubated with horseradish peroxidase-conjugated secondary antibodies (Jackson ImmunoResearch) and visualized using an EzWest-Lumi Plus detection kit (Atto), with detection of luminescence using the LuminoGraph II imaging system (Atto).

2.12 | ELISA

The concentration of TGF-β1 in various culture mediums was quantified using an ELISA kit (#DB100C; R&D Systems) according to the manufacturer's instructions. Each experiment was performed in triplicate.

2.13 | Reanalysis of single-cell RNA sequencing data

Single-cell RNA sequencing (scRNA-seq) data used in this study were obtained from a publicly available dataset, originally published by Karolina Hanna Prazanowska and Su Bin Lim.[27] The Seurat object of the final processed scRNA-seq dataset, including uniform manifold approximation and projection (UMAP) embeddings and precomputed cell cluster assignments, was accessed and downloaded from Figshare (https://doi.org/10.6084/m9.figshare.c.6222221.v3) on 1 July 2023. The Seurat object was loaded into R software (version 4.3.1, R Foundation for Statistical Computing, Vienna, Austria) using the Seurat package (version 4.3.0.1). The data was reanalyzed using the UMAP embeddings and cell identities included in the object. The codes used for the reanalyzes are available as the Data S1.

2.14 | Statistical analysis

Continuous variables were compared using the Student t-test, one- or two-way ANOVA with post-hoc Dunnett test, or Pearson's

correlation coefficient. Categorical variables were compared using a χ^2-test. Overall survival (OS) was defined as the time from the treatment initiation to the date of death from any cause. The Kaplan–Meier method was used to evaluate the probability of OS as a function of time, and differences in time-to-event curves were estimated by log-rank test. The univariable analysis using the Cox regression model was performed to evaluate the effect on survival. Statistical analyses were conducted with SPSS 23.0 for Windows (IBM). All p-values were based on two-tailed statistical analysis, and $p < 0.05$ was considered statistically significant.

3 | RESULTS

3.1 | Distribution and clinical significance of M1-like and M2-like tumor-associated macrophages in lung squamous cell carcinoma

Stromal M1-like TAM density widely ranged among the 221 LUSC TMA specimens (mean ± SD, 432.5 ± 637.3), while islet M1-like TAM density also varied greatly (mean ± SD, 81.0 ± 207.1; Figure 1A,B; Table 1). Stromal M1-like TAM density was significantly correlated with islet M1-like TAM density ($r = 0.309$, $p < 0.0001$). Stromal or islet M1-like TAM density was not associated with clinicopathological factors, including age, gender, Brinkman index, tumor differentiation, tumor size, tumor status, lymph node metastasis, and pathological stage. Cut-off values for stromal M1-like TAM and islet M1-like TAM density were set at the median of 148.0 and 20.0, respectively, due to the lack of association with survival.

 Stromal M2-like TAM density showed a high degree of variation among the 221 LUSC TMA specimens (mean ± SD, 572.9 ± 537.4), while islet M2-like TAM density was also highly variable (mean ± SD, 158.7 ± 242.9; Figure 1C,E; Table 1). Stromal M2-like TAM density was moderately correlated with islet M2-like TAM density ($r = 0.408$, $p < 0.0001$). Stromal M2-like TAM density was significantly associated with tumor size ($p = 0.0420$), tumor status ($p = 0.0300$), and pathological stage ($p = 0.0143$); stromal M2-like TAM density was significantly higher in T3 and T4 tumors than in T1 tumors and in T2 tumors ($p = 0.0352$ and $p = 0.0388$, respectively; Figure 1J); stromal M2-like TAM density was significantly higher in stage III tumors than in stage I tumors ($p = 0.0169$). Islet M2-like TAM density was significantly associated with tumor status ($p = 0.0200$); islet M2-like TAM density was significantly higher in T3 and T4 tumors than in T1 tumors and in T2 tumors ($p = 0.0497$ and $p = 0.0156$, respectively). The optimal cut-off value for stromal M2-like TAM density was 474.4 (area under the curve = 0.582) according to the receiver operating characteristic curve analysis. Consequently, the samples were classified as stromal M2-like TAM-high when stromal M2-like TAM density was >474.4. The cut-off value for islet M2-like TAM density was set at the median of 85.0 because there was no association with survival.

3.2 | M1-like and M2-like tissue microarray status in relation to E-cadherin and vimentin positivity in lung squamous cell carcinoma

The immunohistochemical analysis of TMA specimens for EMT markers showed that 166 (75.1%) tumors were positive for E-cadherin, and 44 (19.9%) were positive for vimentin (Figure 1D,F; Table 2). Stromal or islet M1-like TAM and M2-like TAM status were not associated with positivity for E-cadherin. Stromal or islet M1-like TAM status was not associated with positivity for vimentin. However, stromal M2-like TAM status was significantly associated with positivity for vimentin ($p < 0.0001$), while islet M2-like TAM status was not associated with positivity for vimentin.

3.3 | Prognosis of patients with resected lung squamous cell carcinoma in relation to tumor-associated macrophage status or positivity for E-cadherin and vimentin

There was no significant difference in the OS rate in relation to stromal or islet M1-like TAM status (Figure 2A,B). In contrast, the OS rate was significantly lower in the stromal M2-like TAM-high group than in the stromal M2-like TAM-low group (56.2% vs. 68.5% in 5-year OS; $p = 0.0174$; Figure 2C), although no significant difference was found in the OS rate in relation to islet M2-like TAM status (Figure 2D). There was no significant difference in the OS rate in relation to the positivity for E-cadherin or vimentin (Figure 2E,F).

 The univariable analysis with the Cox regression model showed that stromal M2-like TAM status (hazard ratio = 1.666 [95% confidence interval: 1.089–2.549]; $p = 0.0186$) was a significant predictor for the OS of patients with resected LUSC.

3.4 | Transforming growth factor-β1 expression in the lung cancer microenvironment revealed by reanalysis of scRNA-seq

The reanalysis of the scRNA-seq data demonstrated that TGF-β1 was expressed in a variety of cells in the microenvironment of lung adenocarcinoma (Figure 3A–C). In contrast, within the LUSC microenvironment, TGF-β1 expression was primarily localized to macrophages. These results led us to hypothesize that TGF-β1 derived from TAMs may be promoting EMT in LUSC.

3.5 | H226 and EBC-1 can polarize unstimulated macrophages into tumor-associated macrophages with an M2 phenotype

We applied an in vitro model using human THP-1 monocytes to validate the above clinical results. As shown in the flowchart
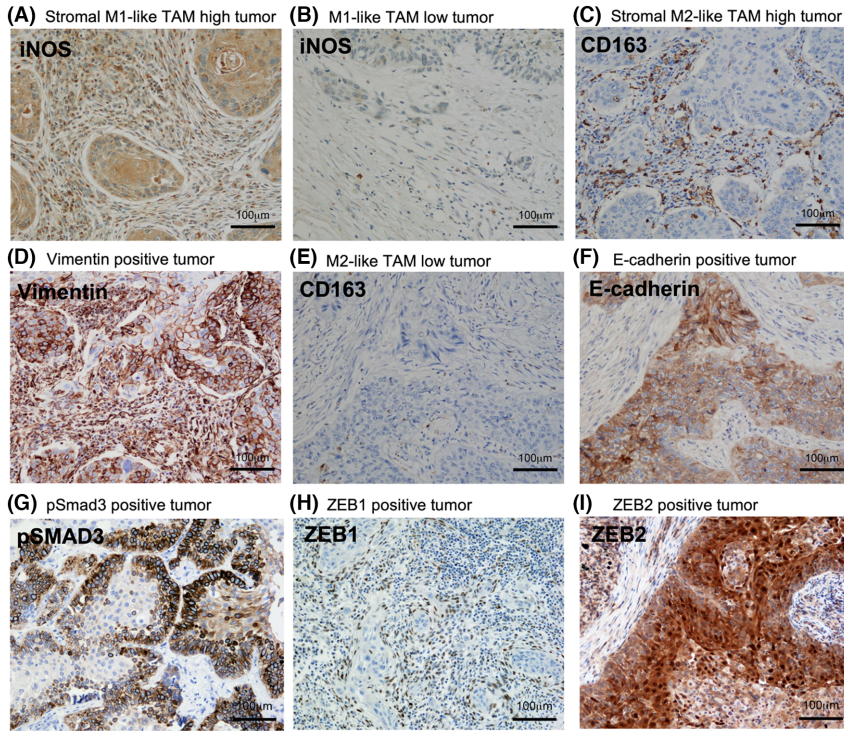
FIGURE 1 Immunostaining of lung squamous cell carcinoma. A squamous cell carcinoma with high density of M1-like TAMs in the tumor stroma and low density of iNOS positive (M1-like) TAMs in the tumor islets (A). A carcinoma with low density of iNOS positive (M1-like) TAMs in the tumor stroma and islets (B). A carcinoma with high density of CD163 positive (M2-like) TAMs in the tumor stroma and low density of CD163 positive (M2-like) TAMs in the tumor islets (C) and with positive vimentin expression in tumor cells (D). A carcinoma with low density of CD163 positive (M2-like) TAMs in the tumor stroma and islets (E) and with positive E-cadherin expression in tumor cells (F). A carcinoma with positive pSmad3 expression in tumor cells (G). A carcinoma with positive ZEB1 expression in tumor cells (H). A carcinoma with positive ZEB2 expression in tumor cells (I). M1-like and M2-like TAM density in the tumor islets and stroma in relation to tumor size, tumor status, nodal status, and pathological status (J). $^*p < 0.05$. Bar, 100 μm. iNOS, inducible nitric oxide synthase; TAM, tumor-associated macrophage.
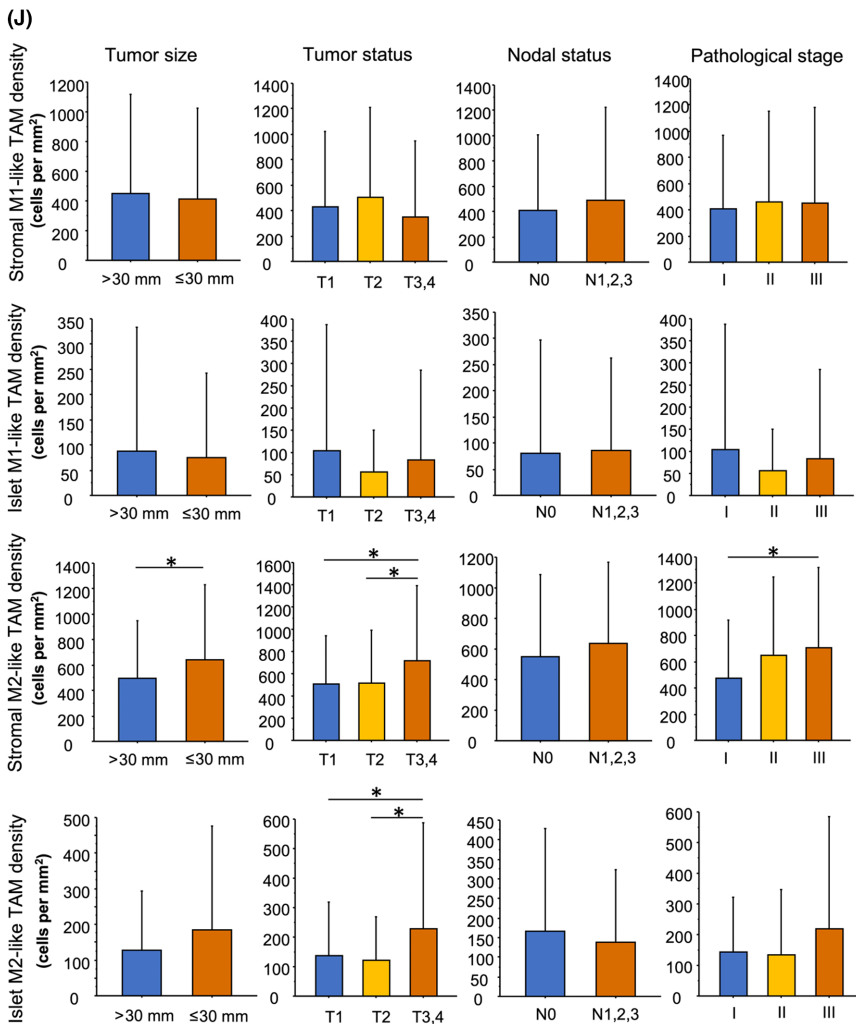
TABLE 1 Distributions of M1-like and M2-like TAMs in patients with lung squamous cell carcinoma according to clinicopathological characteristics.

	n	M1-like TAM density				M2-like TAM density			
		Tumor stroma		Tumor islets		Tumor stroma		Tumor islets	
		Mean±SD (cells per mm²)	p	Mean±SD (cells per mm²)	p	Mean±SD (cells per mm²)	p	Mean±SD (cells per mm²)	p
Age									
≤70	90	493.6±699.1	0.2378[a]	83.1±245.9	0.8993[a]	569.5±518.0	0.9382[a]	167.6±311.8	0.6553[a]
>70	131	390.4±590.1		79.5±176.6		575.2±552.3		152.7±182.1	
Gender									
Female	31	551.2±844.4	0.2642[a]	54.9±105.7	0.4510[a]	411.8±350.4	0.0718[a]	95.6±156.1	0.1185[a]
Male	190	413.1±597.4		85.3±219.2		599.2±558.3		169.0±253.0	
Brinkman index									
≤800	59	452.6±675.6	0.7778[a]	95.7±208.7	0.5264[a]	473.3±488.5	0.0964[a]	163.9±248.7	0.8504[a]
>800	162	425.1±624.7		75.7±206.9		609.2±551.1		156.9±241.4	
Differentiation									
Well	12	227.4±344.8	0.5180[b]	16.7±30.3	0.5436[b]	368.0±253.6	0.3724[b]	165.5±228.4	0.2433[b]
Moderately	142	447.3±628.6		85.2±191.8		575.1±532.8		139.0±175.8	
Poorly	67	437.8±693.9		83.7±251.9		604.9±580.4		199.5±345.5	
Tumor size									
≤30mm	102	452.4±667.3	0.6683[a]	87.4±246.9	0.6715[a]	493.6±452.9	0.0420[a,c]	127.4±168.0	0.0761[a]
>30mm	119	437.8±693.9		75.5±166.5		640.9±593.9		185.6±290.2	
Tumor status									
T1	76	430.5±588.2	0.3866[b]	104.1±282.7	0.3725[b]	508.0±434.8	0.0300[b,c]	138.0±179.3	0.0200[b,c]
T2	79	500.3±710.5		57.3±92.8		513.2±481.2		121.2±148.3	
T3, T4	66	353.5±598.0		82.9±203.4		719.1±671.1		227.6±359.3	
Nodal status									
N0	159	409.8±596.4	0.3984[a]	79.5±218.3	0.8596[a]	547.3±539.0	0.2572[a]	167.1±261.7	0.4163[a]
N1, N2, N3	62	490.6±733.9		85.0±176.7		638.6±532.0		137.4±186.3	
Pathological stage									
I	111	410.0±560.5	0.8693[b]	81.2±236.1	0.7653[b]	470.7±445.7	0.0143[b,c]	143.6±176.8	0.1196[b]
II	59	458.9±696.6		67.4±119.2		648.5±595.9		134.4±211.2	
III	51	450.8±728.5		96.4±221.9		707.9±610.9		219.8±366.0	
Total number	221	432.5±637.3		81.0±207.1		572.9±537.4		158.7±242.9	

Abbreviations: TAM, tumor-associated macrophage.

[a] p-value determined using a t-test.

[b] p-value determined using one-way ANOVA followed by a Dunnett test.

[c] p < 0.05.

TABLE 2 Immunohistochemical evaluation for E-cadherin, vimentin, pSMAD3, ZEB1, and ZEB2 in relation to TAM status in lung squamous cell carcinoma.

	n	Stromal M1-like TAM status			Islet M1-like TAM status			Stromal M2-like TAM status			Islet M2-like TAM status		
		Low	High	p	Low	High	p	Low	High	p	Low	High	p
E-cadherin													
Positive	166	81	85	0.5590[a]	86	80	0.5081[a]	87	79	0.5559[a]	80	86	0.3705[a]
Negative	55	30	25		25	30		32	23		31	24	
Vimentin													
Positive	44	23	21	0.8921[a]	21	23	0.8393[a]	10	34	<0.0001[a,b]	16	28	0.0591[a]
Negative	177	88	89		90	87		109	68		95	82	
pSmad3													
Positive	41	16	25	0.1566[a]	18	23	0.4689[a]	19	22	0.3710[a]	20	21	0.9744[a]
Negative	180	95	85		93	87		100	80		91	89	
ZEB1													
Positive	74	37	37	1.0000[a]	35	39	0.6345[a]	34	40	0.1264[a]	41	33	0.3421[a]
Negative	147	74	73		76	71		85	62		70	77	
ZEB2													
Positive	69	37	32	0.5924[a]	35	34	1.0000[a]	26	43	0.0019[a,b]	30	39	0.2276[a]
Negative	152	74	78		76	76		93	59		81	71	
Total number	221	111	110		111	110		119	102		111	110	

Abbreviation: TAM, tumor-associated macrophage.

[a]p-value determined using χ^2 test.

[b]$p < 0.05$.

(Figure 4A), THP-1 cells were treated with phorbol 12-myristate 13-acetate for 24h for differentiation into unstimulated macrophages. Then, unstimulated macrophages were co-cultured with H226 and EBC-1 for 48h to generate TAMs. Furthermore, unstimulated macrophages were incubated with IL-4 and IL-13 for 48h to generate M2-like macrophages. Consequently, TAMs and M2-like macrophages exhibited higher levels of CD163, CD206, VEGF, and TGF-β1 than unstimulated macrophages by western blotting (Figure 4B). This result demonstrates that TAMs produced by co-culturing THP-1 cells with H226 and EBC-1 cells are M2-phenotype TAMs.

3.6 | Upregulated transforming growth factor-β1 secretion in tumor-associated macrophages co-cultured with H226 and EBC-1 cells

We performed ELISA to measure the TGF-β1 concentration in the culture medium of unstimulated and M2-like macrophages and TAMs co-cultured with H226 or EBC-1 cells. The culture medium was collected after each type of cell had been incubated for 48h. The ELISA results demonstrated a significantly higher TGF-β1 concentration in the culture medium of TAMs co-cultured with H226 (mean±SD, 1.762±0.012ng/mL, $p < 0.0001$) and EBC-1 (mean±SD, 1.887±0.066ng/mL, $p < 0.0001$) and M2-like macrophages (mean±SD, 1.907±0.107ng/mL, $p < 0.0001$) compared

to that of unstimulated macrophages (mean±SD, 0.719±0.002ng/mL; Figure 4C).

These results indicate that TGF-β1 secretion is upregulated in TAMs co-cultured with H226 and EBC-1.

3.7 | Tumor-associated macrophages promote epithelial-mesenchymal transition via the transforming growth factor β/Smad/ZEB pathway in lung squamous cell carcinoma cells

To evaluate the role of TAMs in relation to LUSC cells, H226 and EBC-1 cells were co-cultured with respective TAMs (Figure 5A). Western blotting demonstrated that H226 and EBC-1 cells co-cultured with TAMs exhibited EMT; that is, a decrease in E-cadherin expression and an increase in vimentin expression (Figure 5B). Additionally, levels of pSmad3 were upregulated in H226 and EBC-1 cells co-cultured with TAMs. Regarding EMT-transcription factors, levels of ZEB1 and ZEB2 were increased in H226 cells co-cultured with TAMs, while only ZEB2 was upregulated in EBC-1 cells co-cultured with TAMs. TWIST, Snail, and Slug levels were not increased in H226 or EBC-1 cells co-cultured with TAMs.

Next, we investigated the role of the TGF-β/Smad/ZEB pathway in H226 and EBC-1 cells upon stimulation with TGF-β1 (#781802; BioLegend) at a concentration of 2.5ng/mL for 48h. Furthermore,
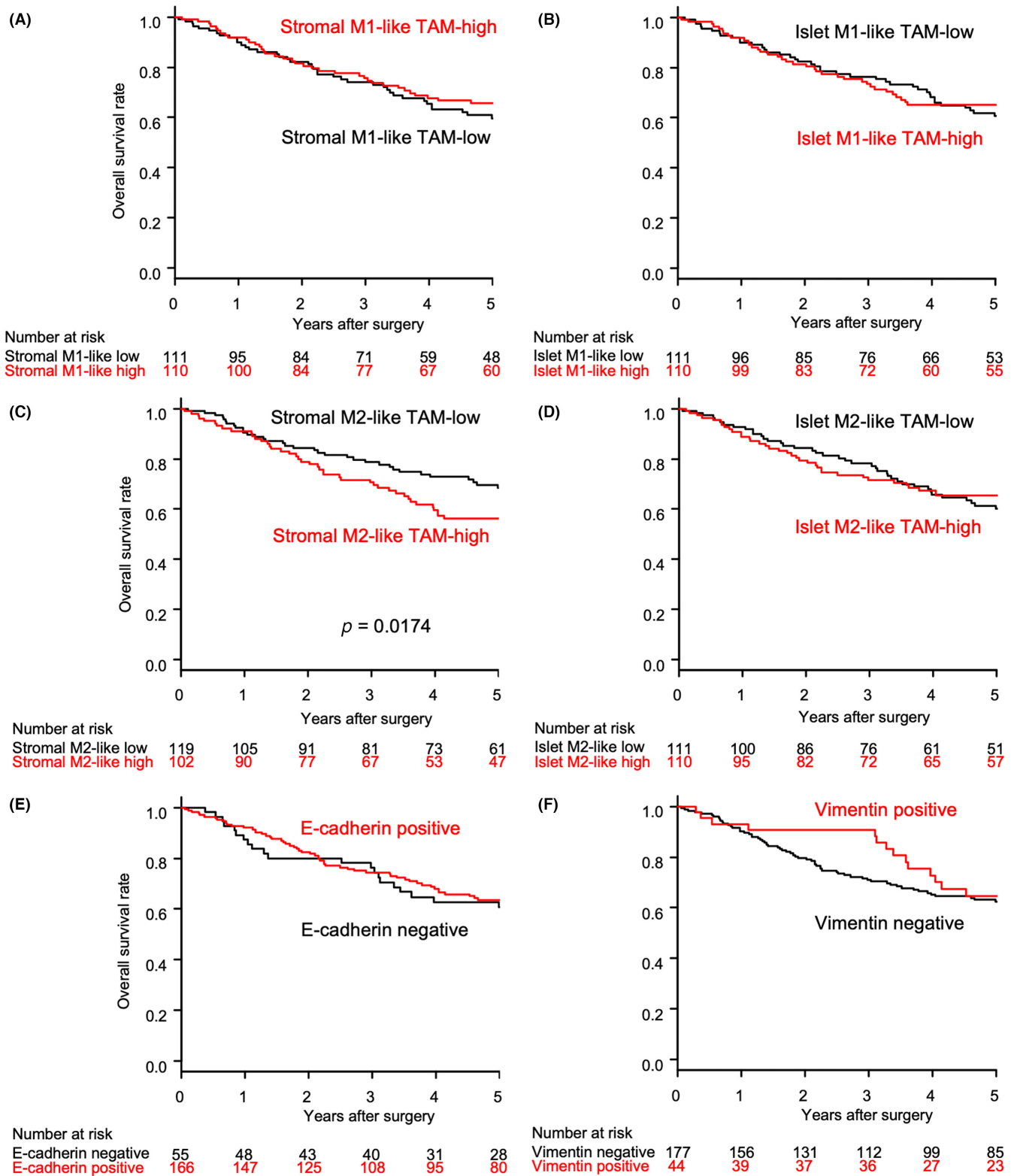
FIGURE 2 Overall survival among patients with resected lung squamous cell carcinoma in relation to (A) stromal M1-like TAM status, (B) islet M1-like TAM status, (C) stromal M2-like TAM status, (D) islet M2-like TAM status, (E) E-cadherin positivity, and (F) vimentin positivity. TAM, tumor-associated macrophage.

we evaluated the effect of RepSox (#S7223; Selleck Chemicals), a TGF-β receptor inhibitor, concurrently applied at 10 μM with TGF-β1 and incubated in the same condition, on this process.

Consequently, TGF-β1 stimulation led to an upregulation of the Smad/ZEB pathway in parental H226 and EBC-1 cells by western blotting (Figure 5C). This activation was accompanied by a
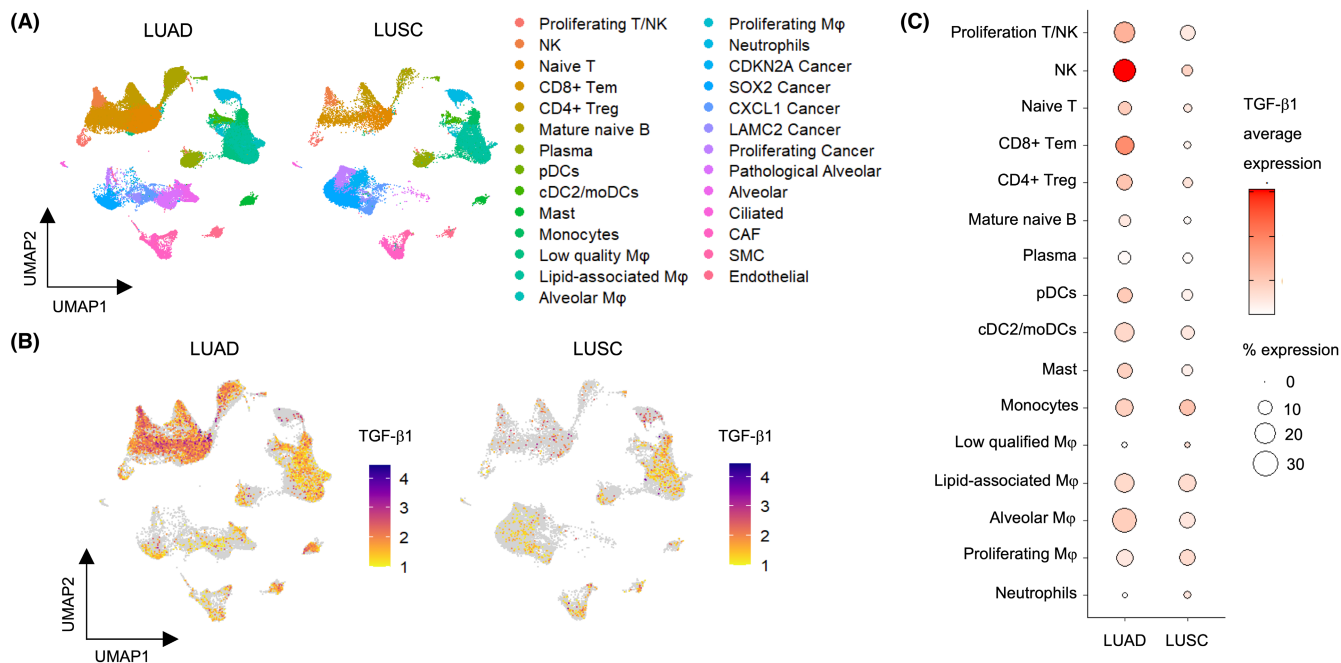
FIGURE 3 TGF-β1 expression in the lung cancer microenvironment revealed by reanalysis of single-cell RNA sequencing data. (A) UMAP showing the distribution of cells in LUAD and LUSC samples. (B) UMAP representation showing the intensity of TGF-β1 expression within all the cell clusters in LUAD and LUSC samples. (C) Dot plots illustrating TGF-β1 expression within immune cell clusters in LUAD and LUSC samples. LUAD, lung adenocarcinoma; LUSC, lung squamous cell carcinoma; Mφ, macrophage; TGF-β1, transforming growth factor β1; UMAP, uniform manifold approximation and projection.
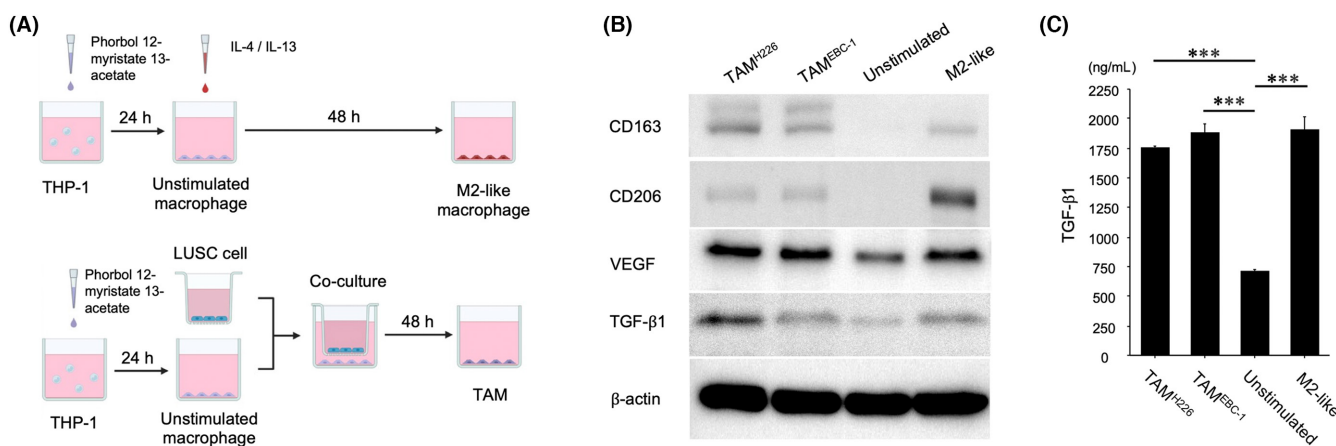
FIGURE 4 TAMs, produced by co-culturing unstimulated macrophages with LUSC cells, are M2-phenotype TAMs that exhibit increased TGF-β1 secretion. (A) Flow chart of the generation of unstimulated and M2-like macrophages and TAMs from THP-1 cells. (B) Western blot analysis of CD163, CD206, VEGF, and TGF-β1 expression in unstimulated and M2-like macrophages and TAMs co-cultured with H226 or EBC-1 cells. (C) TGF-β1 concentration in the culture medium of unstimulated and M2-like macrophages and TAMs co-cultured with H226 or EBC-1 cells, as measured by ELISA. ***$p < 0.001$. ELISA, enzyme-linked immunosorbent assay; LUSC, lung squamous cell carcinoma; TAM, tumor-associated macrophage; TGF-β1, transforming growth factor β1; VEGF, vascular endothelial growth factor.

decrease in E-cadherin expression and an increase in vimentin expression. Furthermore, co-administration of TGF-β1 and RepSox for 48h not only inhibited the activation of the Smad/ZEB pathway observed in TGF-β1-stimulated H226 and EBC-1 cells but also resulted in an increase in E-cadherin expression and a decrease in vimentin expression. Similarly, co-culturing H226 and EBC-1 cells

with respective TAMs in the presence of 10 μM RepSox for 48h also led to inhibition of Smad/ZEB pathway activation, accompanied by increased E-cadherin expression and decreased vimentin expression.

These results indicate that TAMs can induce EMT through the TGF-β/Smad/ZEB pathway in LUSC cells.

3.8 | The WNT signaling pathway is not involved in epithelial-mesenchymal transition of tumor-associated macrophage-co-cultured H226 or EBC-1 cells

Tumor-associated macrophages and M2-like macrophages exhibited higher levels of Wnt5a, a non-canonical Wnt ligand, than unstimulated macrophages by western blotting, while Wnt1, Wnt2b, and Wnt3 were not upregulated (Figure 5D). However, increased levels of phosphorylated CaMKII, a downstream effector of the non-canonical Wnt/Ca²⁺ pathway, were not identified in H226 or EBC-1 cells co-cultured with TAMs (Figure 5E). These results indicate that the WNT signaling pathway is not involved in EMT of TAM-co-cultured H226 or EBC-1 cells.
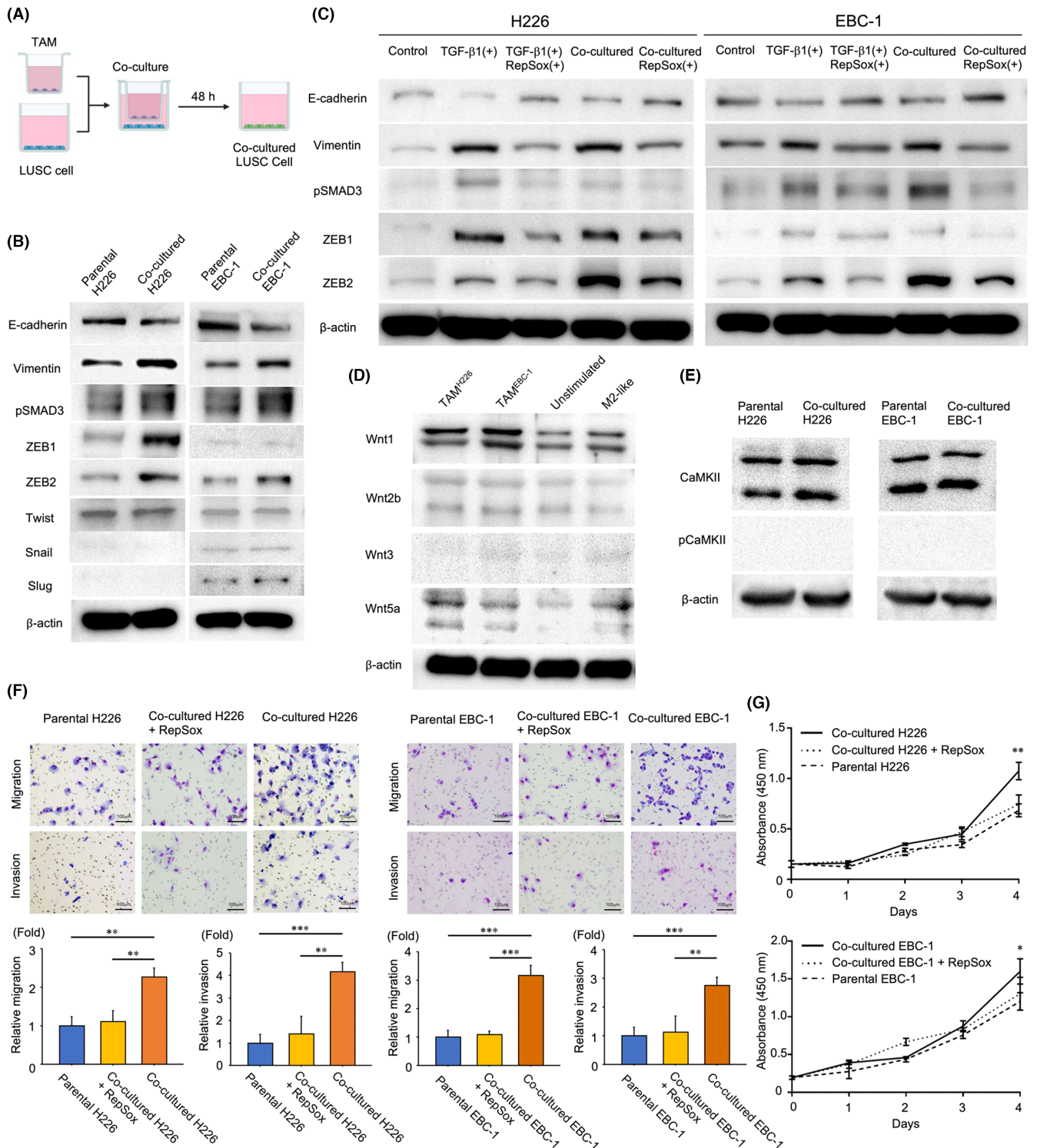

FIGURE 4 (Legend on next page)

FIGURE 5 TAMs can induce EMT through the TGF-β/Smad/ZEB family pathway with enhanced migration and invasion capabilities and improved tumor cell proliferation in LUSC cells. (A) Flow chart of co-culturing LUSC cells with TAMs. (B) Western blot analysis of E-cadherin, vimentin, pSmad3, ZEB1, ZEB2, TWIST, Snail, and Slug expression in co-cultured H226 or EBC-1 cells compared to respective parental cells. (C) Western blot analysis of E-cadherin, vimentin, pSmad3, ZEB1, and ZEB2 expression under five experimental conditions: (1) parental H226 and EBC-1 cells (control), (2) parental H226 and EBC-1 cells stimulated with TGF-β1 (2.5 ng/mL), (3) parental H226 and EBC-1 cells stimulated with TGF-β1 (2.5 ng/mL) and concurrently treated with RepSox (10 μM), (4) H226 and EBC-1 cells co-cultured with TAMs, and (5) H226 and EBC-1 cells co-cultured with TAMs in the presence of RepSox (10 μM). (D) Western blot analysis of Wnt1, Wnt2b, Wnt3, and Wnt5a expression in unstimulated and M2-like macrophages and TAMs co-cultured with H226 or EBC-1 cells. (E) Western blot analysis of CaMKII and phospho-CaMKII expression in co-cultured H226 or EBC-1 cells compared to respective parental cells. (F) Migration and invasion assay analysis comparing parental H226 and EBC-1 cells, those co-cultured with TAMs, and those co-cultured with TAMs in the presence of RepSox (10 μM), using one-way ANOVA with post hoc Dunnett test. Bar, 100 μm. (G) Cell proliferation assay analysis comparing parental H226 and EBC-1 cells, those co-cultured with TAMs, and those co-cultured with TAMs in the presence of RepSox (10 μM), using two-way ANOVA. $*p < 0.05$. $**p < 0.01$. $***p < 0.001$. TAM, tumor-associated macrophage. EMT, epithelial–mesenchymal transition.

3.9 | Tumor-associated macrophages improve migration and invasion capabilities and promote tumor cell proliferation in lung squamous cell carcinoma cells

The migration and invasion assay revealed enhanced migration and invasion capabilities in H226 and EBC-1 cells co-cultured with TAMs compared to parental cells (Figure 5F). The cell proliferation assay analysis showed an improvement in tumor cell proliferation in H226 and EBC-1 cells co-cultured with TAMs compared to parental cells (Figure 5G). Furthermore, H226 and EBC-1 cells, when co-cultured with TAMs in the medium containing 10 μM RepSox for 48 h, displayed reduced migration and invasion capabilities (Figure 5F). H226 and EBC-1 cells co-cultured with TAMs under the same RepSox condition exhibited cell proliferation capacities that fell approximately between those of TAM-co-cultured and parental cells (Figure 5G).

These results indicate that TAMs can improve migration and invasion capabilities and promote tumor cell proliferation in LUSC cells.

3.10 | Immunohistochemical evaluation for pSmad3, ZEB1, and ZEB2 expression in lung squamous cell carcinoma

To validate the in vitro findings, we performed immunohistochemical evaluation for pSmad3, ZEB1, and ZEB2 expression in LUSC. The immunohistochemical analysis of TMA specimens for pSmad3, ZEB1, and ZEB2 showed that 41 (18.6%) tumors were positive for pSmad3, 74 (33.5%) were positive for ZEB1, and 69 (31.2%) were positive for ZEB2 (Figure 2G–I; Table 2). Stromal M2-like TAM status was significantly associated with positivity for ZEB2 ($p = 0.0019$). Moreover, we evaluated the relationships among positivity for E-cadherin, vimentin, pSmad3, ZEB1, and ZEB2 using a χ^2-test (Table S1). Significant associations were observed between vimentin and pSmad3 ($p = 0.0207$), vimentin and ZEB1 ($p < 0.0001$), vimentin and ZEB2 ($p < 0.0001$), pSmad3 and ZEB2 ($p = 0.0124$), and ZEB1 and ZEB2 ($p = 0.0229$). These results provide further evidence for the role of pSmad3, ZEB1, and ZEB2 in the EMT process in LUSC.

4 | DISCUSSION

The present study was performed to elucidate the biological significance of TAMs in relation to EMT in LUSC. Immunohistochemical analyses revealed that M2-like TAM density in the tumor stroma was associated with vimentin expression in LUSC. However, no association was observed between stromal M2-like TAM density and E-cadherin expression. A previous study reported that membranous E-cadherin expression is frequently observed in the tumor center but lost in the invasive front of oral squamous cell carcinomas.[28] Therefore, the lack of association between stromal M2-like TAM density and E-cadherin expression in the present study may be attributed to the fact that TMA cores mainly comprise tissue from the tumor center and contain less or no tissue from the invasive front.

The in vitro experiments in the present study demonstrated that LUSC cells could differentiate unstimulated macrophages into TAMs with an M2 phenotype. These TAMs exhibited higher levels of CD163, CD206, VEGF, TGF-β1, and Wnt5a in western blotting. Additionally, TAMs demonstrated higher TGF-β1 secretion as confirmed by ELISA. CD163, CD206, TGF-β1, and VEGF are well-known markers for M2-like TAMs.[11,29] While unstimulated macrophages can be differentiated into TAMs with an M2 phenotype by internalizing lung tumor cell-derived exosomes,[30] experimental studies have demonstrated that the Wnt signaling pathway could be important for the M2-like polarization of TAMs.[31–33] Wnt5a secreted from TAMs stimulates macrophages to secrete IL-10, which acts in a paracrine and autocrine manner to accelerate M2-like polarization.[33] Our previous clinical study showed that Wnt5a expression in the tumor cells and stromal cells was associated with M2-like TAM density in the tumor stroma in non-small cell lung cancer.[34]

Furthermore, the present study clearly demonstrated that TAMs could induce EMT via the TGF-β/Smad/ZEB pathway in LUSC cells. Upon binding of TGF-β with the TGF-β receptor, Smad2 and Smad3 are phosphorylated, forming a complex with Smad4 that translocates into the nucleus to initiate transcription of EMT-transcription factors genes.[35] In the present study, the expression levels of ZEB family proteins were upregulated in LUSC cells co-cultured with TAMs. Meanwhile, we observed upregulation of Wnt5a expression in TAMs. Although the Wnt signaling pathway plays a role in the communication between tumor and stroma in the tumor microenvironment,[36]

we could not detect activation of the non-canonical Wnt signaling pathway, which is known to induce EMT, in LUSC cells co-cultured with TAMs in the present study. This finding was confirmed by the absence of CaMKII phosphorylation, a downstream effector of the non-canonical Wnt pathway, in co-cultured LUSC cells. To the best of our knowledge, this study is the first to demonstrate the significance of the TGF-β/Smad/ZEB pathway with respect to EMT induced by TAMs in LUSC cells. Moreover, the migration and invasion assay verified the enhanced capabilities of migration and invasion in LUSC cells co-cultured with TAMs.

In addition, LUSC cells co-cultured with TAMs exhibited improved tumor cell proliferation. This effect is likely due to various growth factors, including VEGF, secreted by TAMs.[11] In contrast, recent studies have suggested an association between EMT and chemoresistance,[37–39] although the mechanism of chemoresistance can differ depending on the type of chemotherapeutic agent used. These findings may partly explain why the OS rate in patients with resected LUSC was lower in the stromal M2-like TAM-high group than in the stromal M2-like TAM-low group in the present study.

This study has some limitations. First, the immunohistochemical evaluation was based on TMA, which may not capture the full heterogeneity of the original tissue sample. Second, this study employed a non-contact two-dimensional co-culture system, which may not accurately reflect the complex interactions between tumor cells and their microenvironment in vivo. Third, although THP-1 cells can differentiate into macrophage-like cells, they do not necessarily replicate the behavior exhibited by primary human macrophages.

In conclusion, the present study demonstrated that TAMs could induce EMT with increased metastatic potential and tumor cell proliferation in LUSC, leading to a poor prognosis. Therefore, TAMs are considered a promising therapeutic target for LUSC. M2-like TAM-targeted therapy might be more effective against LUSC than lung adenocarcinoma because M2-like TAM density in LUSC is higher than that in lung adenocarcinoma.[5] Further investigations are necessary to develop promising treatment strategies against LUSC, such as reprogramming TAMs into an anti-tumor phenotype[40,41] and inhibiting EMT.[42–44]

AUTHOR CONTRIBUTIONS

Ryota Sumitomo, Toshi Menju, and Hiroshi Date designed the study. Ryota Sumitomo, Toshi Menju, Shimazu Yumeta, Toshiya Toyazaki, Hideaki Miyamoto, and Naohisa Chiba collected the data and performed the experiments. Ryota Sumitomo, Toshi Menju, Yutaka Hirayama, and Atsuyasu Sato analyzed and interpreted the data. Ryota Sumitomo and Toshi Menju wrote the manuscript. All authors reviewed and revised the manuscript. The final manuscript was read and approved by all authors.

ACKNOWLEDGMENTS

Not applicable.

CONFLICT OF INTEREST STATEMENT

The authors have no conflicts of interest to declare.

ETHICS STATEMENT

Approval of the research protocol by an Institutional Reviewer Board: The study was approved by the Ethics Committee of the hospital (approval no. R1706).
Informed Consent: Written informed consent was provided by each patient.
Registry and the Registration No. of the study/trial: N/A.
Animal Studies: N/A.

ORCID

Ryota Sumitomo https://orcid.org/0000-0002-1676-1571

REFERENCES

1. Perez-Moreno P, Brambilla E, Thomas R, Soria JC. Squamous cell carcinoma of the lung: molecular subtypes and therapeutic opportunities. *Clin Cancer Res*. 2012;18:2443-2451.
2. Billena C, Lobbous M, Cordova CA, et al. The role of targeted therapy and immune therapy in the management of non-small cell lung cancer brain metastases. *Front Oncol*. 2023;13:1110440. doi:10.3389/fonc.2023.1110440
3. Garon EB, Rizvi NA, Hui R, et al. Pembrolizumab for the treatment of non-small-cell lung cancer. *N Engl J Med*. 2015;372:2018-2028. doi:10.1056/NEJMoa1501824
4. Hirsch FR, Scagliotti GV, Mulshine JL, et al. Lung cancer: current therapies and new targeted treatments. *Lancet*. 2017;389:299-311. doi:10.1016/S0140-6736(16)30958-8
5. Sumitomo R, Hirai T, Fujita M, Murakami H, Otake Y, Huang CL. M2 tumor-associated macrophages promote tumor progression in non-small-cell lung cancer. *Exp Ther Med*. 2019;18:4490-4498. doi:10.3892/etm.2019.8068
6. Sumitomo R, Hirai T, Fujita M, Murakami H, Otake Y, Huang CL. PD-L1 expression on tumor-infiltrating immune cells is highly associated with M2 TAM and aggressive malignant potential in patients with resected non-small cell lung cancer. *Lung Cancer*. 2019;136:136-144. doi:10.1016/j.lungcan.2019.08.023
7. Sumitomo R, Huang CL, Fujita M, Cho H, Date H. Differential expression of PD-L1 and PD-L2 is associated with the tumor microenvironment of TILs and M2 TAMs and tumor differentiation in non-small cell lung cancer. *Oncol Rep*. 2022;47:73. doi:10.3892/or.2022.8284
8. Mei J, Xiao Z, Guo C, et al. Prognostic impact of tumor-associated macrophage infiltration in non-small cell lung cancer: a systemic review and meta-analysis. *Oncotarget*. 2016;7:34217-34228. doi:10.18632/oncotarget.9079
9. Jackute J, Zemaitis M, Pranys D, et al. Distribution of M1 and M2 macrophages in tumor islets and stroma in relation to prognosis of non-small cell lung cancer. *BMC Immunol*. 2018;19:3. doi:10.1186/s12865-018-0241-4
10. van Dalen FJ, van Stevendaal MHME, Fennemann FL, Verdoes M, Ilina O. Molecular repolarisation of tumour-associated macrophages. *Molecules*. 2018;24:9. doi:10.3390/molecules24010009
11. Li X, Chen L, Peng X, Zhan X. Progress of tumor-associated macrophages in the epithelial-mesenchymal transition of tumor. *Front Oncol*. 2022;12:911410. doi:10.3389/fonc.2022.911410
12. Neri S, Menju T, Sowa T, et al. Prognostic impact of microscopic vessel invasion and visceral pleural invasion and their correlations with epithelial-mesenchymal transition, cancer stemness, and treatment failure in lung adenocarcinoma. *Lung Cancer*. 2019;128:13-19. doi:10.1016/j.lungcan.2018.12.001

13. Lamouille S, Xu J, Derynck R. Molecular mechanisms of epithelial-mesenchymal transition. *Nat Rev Mol Cell Biol.* 2014;15:178-196. doi:10.1038/nrm3758

14. Nieto MA, Huang RY, Jackson RA, Thiery JP. EMT: 2016. *Cell.* 2016;166:21-45. doi:10.1016/j.cell.2016.06.028

15. Xu J, Lamouille S, Derynck R. TGF-beta-induced epithelial to mesenchymal transition. *Cell Res.* 2009;19:156-172. doi:10.1038/cr.2009.5

16. Yin P, Bai Y, Wang Z, et al. Non-canonical Fzd7 signaling contributes to breast cancer mesenchymal-like stemness involving Col6a1. *Cell Commun Signal.* 2020;18:143. doi:10.1186/s12964-020-00646-2

17. Alonso-Nocelo M, Raimondo TM, Vining KH, López-López R, de la Fuente M, Mooney DJ. Matrix stiffness and tumor-associated macrophages modulate epithelial to mesenchymal transition of human adenocarcinoma cells. *Biofabrication.* 2018;10:035004. doi:10.1088/1758-5090/aaafbc

18. Wang J, Wang N, Zheng Z, et al. Exosomal lncRNA HOTAIR induce macrophages to M2 polarization via PI3K/ p-AKT /AKT pathway and promote EMT and metastasis in laryngeal squamous cell carcinoma. *BMC Cancer.* 2022;22:1208. doi:10.1186/s12885-022-10210-5

19. Song J, Yang P, Li X, et al. Esophageal cancer-derived extracellular vesicle miR-21-5p contributes to EMT of ESCC cells by disorganizing macrophage polarization. *Cancers (Basel).* 2021;13:4122. doi:10.3390/cancers13164122

20. She L, Qin Y, Wang J, et al. Tumor-associated macrophages derived CCL18 promotes metastasis in squamous cell carcinoma of the head and neck. *Cancer Cell Int.* 2018;18:120. doi:10.1186/s12935-018-0620-1

21. Gao L, Zhang W, Zhong WQ, et al. Tumor associated macrophages induce epithelial to mesenchymal transition via the EGFR/ERK1/2 pathway in head and neck squamous cell carcinoma. *Oncol Rep.* 2018;40:2558-2572. doi:10.3892/or.2018.6657

22. You Y, Tian Z, Du Z, et al. M1-like tumor-associated macrophages cascade a mesenchymal/stem-like phenotype of oral squamous cell carcinoma via the IL6/Stat3/THBS1 feedback loop. *J Exp Clin Cancer Res.* 2022;41:10. doi:10.1186/s13046-021-02222-z

23. Amin MB, Edge S, Greene F. *AJCC Cancer Staging Manual.* 8th ed. Springer; 2017.

24. Travis WD, Brambilla E, Burke AP, Marx A, Nicholson AG. *WHO Classification of Tumours of the Lung, Pleura, Thymus and Heart.* 4th ed. International Agency for Research on Cancer; 2015.

25. Kononen J, Bubendorf L, Kallioniemi A, et al. Tissue microarrays for high-throughput molecular profiling of tumor specimens. *Nat Med.* 1998;4:844-847. doi:10.1038/nm0798-844

26. Sowa T, Menju T, Sonobe M, et al. Association between epithelial-mesenchymal transition and cancer stemness and their effect on the prognosis of lung adenocarcinoma. *Cancer Med.* 2015;4:1853-1862. doi:10.1002/cam4.556

27. Prazanowska KH, Lim SB. An integrated single-cell transcriptomic dataset for non-small cell lung cancer. *Sci Data.* 2023;10:167. doi:10.1038/s41597-023-02074-6

28. Attramadal CG, Kumar S, Boysen ME, Dhakal HP, Nesland JM, Bryne M. Tumor budding, EMT and cancer stem cells in T1-2/N0 Oral squamous cell carcinomas. *Anticancer Res.* 2015;35:6111-6120.

29. Okikawa S, Morine Y, Saito Y, et al. Inhibition of the VEGF signaling pathway attenuates tumor-associated macrophage activity in liver cancer. *Oncol Rep.* 2022;47:71. doi:10.3892/or.2022.8282

30. Pritchard A, Tousif S, Wang Y, et al. Lung tumor cell-derived exosomes promote M2 macrophage polarization. *Cell.* 2020;9:1303. doi:10.3390/cells9051303

31. Jiang Y, Han Q, Zhao H, Zhang J. Promotion of epithelial-mesenchymal transformation by hepatocellular carcinoma-educated macrophages through Wnt2b/β-catenin/c-Myc signaling and reprogramming glycolysis. *J Exp Clin Cancer Res.* 2021;40:13. doi:10.1186/s13046-020-01808-3

32. Tian X, Wu Y, Yang Y, et al. Long noncoding RNA LINC00662 promotes M2 macrophage polarization and hepatocellular carcinoma progression via activating Wnt/β-catenin signaling. *Mol Oncol.* 2020;14:462-483. doi:10.1002/1878-0261.12606

33. Liu Q, Yang C, Wang S, et al. Wnt5a-induced M2 polarization of tumor-associated macrophages via IL-10 promotes colorectal cancer progression. *Cell Commun Signal.* 2020;18:51. doi:10.1186/s12964-020-00557-2

34. Sumitomo R, Huang CL, Ando H, Ishida T, Cho H, Date H. Wnt2b and Wnt5a expression is highly associated with M2 TAMs in non-small cell lung cancer. *Oncol Rep.* 2022;48:189. doi:10.3892/or.2022.8404

35. Menju T, Date H. Lung cancer and epithelial-mesenchymal transition. *Gen Thorac Cardiovasc Surg.* 2021;69:781-789. doi:10.1007/s11748-021-01595-4

36. Huang CL, Liu D, Nakano J, et al. Wnt5a expression is associated with the tumor proliferation and the stromal vascular endothelial growth factor–An expression in non-small-cell lung cancer. *J Clin Oncol.* 2005;23:8765-8773. doi:10.1200/JCO.2005.02.2871

37. Kuwada K, Kagawa S, Yoshida R, et al. The epithelial-to-mesenchymal transition induced by tumor-associated macrophages confers chemoresistance in peritoneally disseminated pancreatic cancer. *J Exp Clin Cancer Res.* 2018;37:307. doi:10.1186/s13046-018-0981-2

38. Toge M, Yokoyama S, Kato S, et al. Critical contribution of MCL-1 in EMT-associated chemo-resistance in A549 non-small cell lung cancer. *Int J Oncol.* 2015;46:1844-1848. doi:10.3892/ijo.2015.2861

39. Fukuda K, Takeuchi S, Arai S, et al. Epithelial-to-mesenchymal transition is a mechanism of ALK inhibitor resistance in lung cancer independent of ALK mutation status. *Cancer Res.* 2019;79:1658-1670. doi:10.1158/0008-5472.CAN-18-2052

40. Jaynes JM, Sable R, Ronzetti M, et al. Mannose receptor (CD206) activation in tumor-associated macrophages enhances adaptive and innate antitumor immune responses. *Sci Transl Med.* 2020;12:eaax6337. doi:10.1126/scitranslmed.aax6337

41. Giurisato E, Xu Q, Lonardi S, et al. Myeloid ERK5 deficiency suppresses tumor growth by blocking protumor macrophage polarization via STAT3 inhibition. *Proc Natl Acad Sci USA.* 2018;115:E2801-E2810. doi:10.1073/pnas.1707929115

42. Takahashi K, Menju T, Nishikawa S, et al. Tranilast inhibits TGF-β1-induced epithelial-mesenchymal transition and invasion/metastasis via the suppression of Smad4 in human lung cancer cell lines. *Anticancer Res.* 2020;40:3287-3296. doi:10.21873/anticanres.14311

43. Nishikawa S, Menju T, Takahashi K, et al. Statins may have double-edged effects in patients with lung adenocarcinoma after lung resection. *Cancer Manag Res.* 2019;11:3419-3432. doi:10.2147/CMAR.S200819

44. Ishikawa H, Menju T, Toyazaki T, et al. A novel cell-based assay for the high-throughput screening of epithelial-mesenchymal transition inhibitors: identification of approved and investigational drugs that inhibit epithelial-mesenchymal transition. *Lung Cancer.* 2023;175:36-46. doi:10.1016/j.lungcan.2022.11.015

SUPPORTING INFORMATION

Additional supporting information can be found online in the Supporting Information section at the end of this article.